J Physiol 595.11 (2017) pp 3361–3376

The Journal of Physiology

SIRT1 may play a crucial role in overload-induced hypertrophy of skeletal muscle

Erika Koltai[1], Zoltán Bori[1], Clovis Chabert[2], Hervé Dubouchaud[2], Hisashi Naito[3], Shuichi Machida[3], Kelvin JA Davies[4], Zsolt Murlasits[5], Andrew C Fry[6], Istvan Boldogh[7] and Zsolt Radak[1,8]

[1]*Research Institute of Sport Science, University of Physical Education, Budapest, Hungary*
[2]*Université Joseph Fourier, Laboratoire de Bioénergétique Fondamentale et Appliquée, Grenoble Cedex 0938041, France*
[3]*Department of Exercise Physiology, Graduate School of Health and Sports Science & Medicine, Juntendo University, Japan*
[4]*Ethel Percy Andrus Gerontology Centre of the Leonard Davis School of Gerontology; and Division of Molecular & Computational Biology, Department of Biological Sciences, of the Dornsife College of Letters, Arts, and Sciences, the University of Southern California, Los Angeles, CA 90089-0191, USA*
[5]*Sport Science Program, Qatar University, Doha, Qatar*
[6]*Osness Human Performance Laboratories, Department of Health, Sport, and Exercise Sciences, University of Kansas, Lawrence, KS 66045, USA*
[7]*Department of Microbiology and Immunology, University of Texas Medical Branch at Galveston, Galveston, TX 77555, USA*
[8]*Institute of Sport Sciences and Physical Education, University of Pecs, Pecs, Hungary*

Key points

- Silent mating type information regulation 2 homologue 1 (SIRT1) activity and content increased significantly in overload-induced hypertrophy.
- SIRT1-mediated signalling through Akt, the endothelial nitric oxide synthase mediated pathway, regulates anabolic process in the hypertrophy of skeletal muscle.
- The regulation of catabolic signalling via forkhead box O 1 and protein ubiquitination is SIRT1 dependent.
- Overload-induced changes in microRNA levels regulate SIRT1 and insulin-like growth factor 1 signalling.

Abstract Significant skeletal muscle mass guarantees functional wellbeing and is important for high level performance in many sports. Although the molecular mechanism for skeletal muscle hypertrophy has been well studied, it still is not completely understood. In the present study, we used a functional overload model to induce plantaris muscle hypertrophy by surgically removing the soleus and gastrocnemius muscles in rats. Two weeks of muscle ablation resulted in a 40% increase in muscle mass, which was associated with a significant increase in silent mating type information regulation 2 homologue 1 (SIRT1) content and activity ($P < 0.001$). SIRT1-regulated Akt, endothelial nitric oxide synthase and GLUT4 levels were also induced in hypertrophied muscles, and SIRT1 levels correlated with muscle mass, paired box protein 7 (Pax7), proliferating cell nuclear antigen (PCNA) and nicotinamide phosphoribosyltransferase (Nampt) levels. Alternatively, decreased forkhead box O 1 (FOXO1) and increased K48 poly-ubiquitination also suggest that SIRT1 could be involved in the catabolic process of hypertrophy. Furthermore, increased levels of K63 and muscle RING finger 2 (MuRF2) protein could also be important enhancers of muscle mass. We report here that the levels of miR1 and miR133a decrease in hypertrophy and negatively correlate with muscle mass, SIRT1 and Nampt levels. Our results reveal a strong correlation between SIRT1 levels and activity, SIRT1-regulated pathways and overload-induced hypertrophy. These findings, along with the well-known regulatory roles that SIRT1 plays in modulating both anabolic and catabolic pathways, allow us to propose the hypothesis that SIRT1 may actually play a crucial causal role in overload-induced hypertrophy of skeletal muscle. This hypothesis will now require rigorous direct and functional testing.

DOI: 10.1113/JP273774

(Received 13 November 2016; accepted after revision 23 February 2017; first published online 2 March 2017)
Corresponding author Z. Radak: Institute of Sport Science, University of Physical Education, Alkotas u. 44.TF Budapest, Hungary. Email: radak@tf.hu

Abbreviations cIAPs, cellular inhibitor of apoptosis protein; dNTP, deoxynucleoside triphosphate; EAAs, essential amino acids; eNOS, endothelial nitric oxide synthase; Erk, extracellular signal-regulated kinase; FOXO1, forkhead box O 1; Fstl1, follistatin-like 1; GAPDH, glyceraldehyde 3-phosphate dehydrogenase; H_2DCFDA, dichlorodihydrofluorescein diacetate; IGF-1, insulin-like growth factor 1; iNOS, inducible nitric oxide synthase; MAPK, mitogen-activated protein kinase; miRNA/miR, microRNA; mTOR, mammalian target of rapamycin; mTORC1, mammalian target of rapamycin complex 1; MuRF, muscle RING finger; NAM, nicotinamide; Nampt, nicotinamide phosphoribosyltransferase; NF-kB, nuclear factor kappa B; NGS, normal goat serum; NOX4, NADPH oxidase 4; PARP-1, poly [ADP-ribose] polymerase; Pax7, paired box protein 7; PCNA, proliferating cell nuclear antigen; PGC1-α, peroxisome proliferator-activated receptor gamma coactivator 1-α; PSMA6, proteasome subunit alpha type-6; PVDF, polyvinylidene difluoride; qRT-PCR, quantitative real-time reverse-transcription PCR; ROS, reactive oxygen species; SIRT1, silent mating type information regulation 2 homologue 1; TBST, Tris-buffered saline-Tween-20; Ub, ubiquitin; XIAP, X-linked inhibitor of apoptosis protein.

Introduction

Skeletal muscle is a dynamic organ that can change its metabolic rate many fold during intensive contractions. This organ reacts well to endurance training by increasing mitochondrial biogenesis, promoting capillarization, and enhancing oxidative enzyme activities (Holloszy, 1967; Davies *et al.* 1981; Marton *et al.* 2015). Due to the dynamic characteristics of skeletal muscle, bed rest, immobilization, ageing and different types of muscle diseases often result in muscle atrophy. Since muscle mass is closely related to force-generating capacity (Goldspink, 1999), training that stimulates hypertrophy is often used in elite sports to enhance performance, or in recreational activities, to improve quality of life.

The increase in multi-nucleated myocytes that results from resistance training can also readily bring about an increase in size. Hypertrophy requires the activation of anabolic processes and also, possibly, the suppression of catabolic processes. Exercise of a relatively high load can often lead to micro trauma, due to high tension. This, in turn, activates satellite cells resulting in efficient tissue repair, which could be one of the initiating steps of muscle hypertrophy (Viles & Powell, 1981; Shepstone *et al.* 2005). During the activation of stem cells or satellite cells, there is an increased energy requirement to synthesize macromolecules and maintain an acceptable level of autophagy (Tang & Rando, 2014). Because silent mating type information regulation 2 homologue 1 (SIRT1) is one of the regulators of autophagy, down-regulation of SIRT1 delays activation of satellite cells and probably the regeneration of skeletal muscle (Tang & Rando, 2014). Indeed, SIRT1 has been shown to regulate energy metabolism during myogenesis (Nedachi *et al.* 2008). The acetylation levels of H4K16 can readily affect the transcription of certain muscle-specific genes, and these lysine residues are deacetylated by SIRT1. It is reported that inactivation of SIRT1 deacetylase activity results in reduced myofibre size, as well as in regeneration and depression of certain genes important to muscle development (Ryall *et al.* 2015).

SIRT1 is a sensitive modulator of metabolic processes, regulating fat and sugar metabolism (Canto *et al.* 2009; Han *et al.* 2013; Banerjee *et al.* 2016). Generally, it is believed that SIRT1 is activated during caloric restriction, when anabolic pathways are down-regulated. However, the results of a recent study indicate that SIRT1 could increase protein synthesis in a cell type-dependent manner, through mammalian target of rapamycin complex 1 (mTORC1) signalling (Igarashi & Guarente, 2016).

SIRT1 can also interact with peroxisome proliferator-activated receptor gamma coactivator (PGC-1α), which is the master regulator of mitochondrial biogenesis. The results of a recent study suggest that hypertrophy and mitochondrial biogenesis can occur simultaneously (Scheffler *et al.* 2014) although the increases in mitochondrial mass are not associated with increased aerobic capacity (Scheffler *et al.* 2014). It is generally believed that activation of PGC-1α is an adaptive response to endurance training, but apparently resistance training can also activate PGC-1α via one of the isoforms of this co-activator. It is well known that the activation of PGC-1α is isoform-specific (Yoshioka *et al.* 2009) as is regulation of the *PGC-1α1*, *PGC-1α2* and *PGC-1α3* genes, while the *PGC-1α4* gene exhibits a very different regulation profile (Ruas *et al.* 2012). *PGC-1α4* shares the same alternative exon1 with *PGC-1α2* and has the same N-terminus, but its mRNA structure is different as it contains a 31 nucleotide insertion between exons 6 and 7, which generates a premature stop codon. Moreover, *PGC1α4* encodes a 266 amino acid protein whose molecular weight is 29.1 kDa, whereas the molecular weights of other PGC1-α protein isoforms are all around 41 kDa. Interestingly, insulin-like growth factor 1 (IGF-1) and mammalian target of rapamycin (mTOR) pathways, which are very important for muscle hypertrophy, are activated

by PGC-1α4. It was indicated that both endurance and resistance training have to activate PGC-1α, which appears to be the ultimate exercise-regulated protein (Ruas *et al.* 2012).

In addition to the PGC-1α–SIRT1 interaction, SIRT1 can also influence nitric oxide (NO) signalling and endothelial nitric oxide synthase (eNOS) activity, which is regulated by acetylation/deacetylation, and SIRT1 has been shown to deacetylate K496 and K506 in the structure of eNOS (Mattagajasingh *et al.* 2007). The SIRT1-mediated upregulation of eNOS can induce mitochondrial biogenesis (Csiszar *et al.* 2009) and NO is also important for the proliferation of satellite cells (Anderson, 2000). Moreover, NO mediates the signalling cascade via guanylate cyclase and the generation of cyclic guanosine monophosphate (cGMP) can induce follistatin expression (Pisconti *et al.* 2006), which can also affect muscle hypertrophy. Follistatin is an antagonist of myostatin, which is a negative regulator of skeletal muscle mass. Indeed, activation of follistatin has been shown to inhibit the activity of myostatin and result in hypertrophy (Lee & McPherron, 2001). Moreover, follistatin-like 1 (Fstl1) protein, which belongs to the follistatin family, can activate Akt/eNOS signalling and modulate protein synthesis (Ouchi *et al.* 2008).

The need for increased protein synthesis during muscle hypertrophy is associated with a significant activation of muscle-specific genes and large increases in mRNA levels. However, not all mRNAs transcribed result in protein assembly, due to the many different post-transcriptional control systems that exist in cells.

MicroRNAs (miRNAs) are short, single stranded, non-coding RNA molecules that negatively regulate their targets at the post-transcriptional level by pairing their nucleotides 2–8 at the 5′ end, leading to either mRNA degradation or translational repression. It is suggested that miRNAs could play a crucial role in skeletal muscle development, and myogenesis (Lu *et al.* 2012). MirR1, as an inhibitory molecule, suppresses the activity of the transcriptional regulator, histone deacetylase 4, which increases the activity of myocyte enhancer factor-2 which, in turn, facilitates cellular differentiation (Rao *et al.* 2006). In addition, MyoD appears to suppress the expression of some genes, including Fstl1, by the activation of muscle- specific miR-206 (Rosenberg *et al.* 2006). Down-regulation of miR-133 resulted in increased muscle fibre size and force generation following electrical stimulation of skeletal muscle (Rhim *et al.* 2010), indicating the importance of this miR in muscle function. Also, SIRT1, which is a potential regulator of muscle hypertrophy, is controlled by miRs (Buler *et al.* 2016).

In the present study, we investigated the role of SIRT1 in overload-induced muscle hypertrophy in order to clarify the importance of some molecular pathways and interactions with signalling processes.

Methods

Animals

Middle aged (15 months) male Wistar rats (507 $\pm$ 33 g) from the animal facility of the Research Institute of Sport Science, University of Physical Education, were used in the study and assigned to control ($n = 6$) and hypertrophied ($n = 7$) groups. Animals were housed in a thermoneutral environment (~22°C), on a 12:12 h photoperiod, and were provided with food and water *ad libitum*. The investigation was carried out according to the requirements of *The Guiding Principles for Care and Use of Animals*, EU, and approved by the local ethics committee, also conforming to the principles of UK regulations, as described in Grundy (2015).

Muscle overload

All surgical procedures were performed under aseptic conditions with the animals deeply anaesthetized with pentobarbital sodium (50 mg kg^{-1} I.P.). Analgetics (doliprane at a dose of 500 mg l^{-1} in drinking water) was administered to the animals for 2 days following the operation. Compensatory overload of the plantaris muscle was performed bilaterally via removal of their major synergistic muscles (gastrocnemius-medialis, -lateralis and soleus), as described in detail previously (Baldwin *et al.* 1982; Bigard *et al.* 2001; Chaillou *et al.* 2012). Particular attention was made to ensure that plantaris neural and vascular supplies were not damaged, and the aponeuroses and skin were independently sutured. A sham operation was systematically performed in control, non-overloaded groups, which consisted of separating tendons of the soleus and gastrocnemius muscles from that of the plantaris muscle. The overload lasted for 14 days and the animals were continuously monitored throughout the experimental period. At end of the overload period the rats were killed via decapitation. The plantaris muscle was carefully and quickly removed bilaterally, trimmed of excess fat and connective tissue, wet weighed, frozen in liquid nitrogen and stored at −80°C until subsequent analysis.

Immunohistochemistry

Deparaffinized and rehydrated muscle sections were autoclaved for 5 min in 10 mM sodium citrate (pH 6.0) for antigen retrieval. Endogenous peroxidase was inactivated by incubation in 0.3% H_2O_2 in methanol for 30 min on ice. After blocking in 10% normal goat serum (NGS), 2% BSA, 0.1% Triton-X100 in PBS for 30 min at room temperature, the sections were incubated with anti-Pax7 mouse monoclonal antibody (Development Studies Hybridoma Bank, Iowa City, IA, USA) diluted 1:3 with 2% BSA in PBS at 37°C for 1 h. After washing with cold PBS, four times,

sections were incubated with anti-mouse HRP-conjugated sheep secondary antibody (GE Healthcare, Piscataway, NJ, USA: NA931V) diluted 1:200 with 10% NGS, 2% BSA in PBS. Following washing with cold PBS, four times, ImmPACT DAB substrate kit (Vector Laboratories, Burlingame, CA, USA: SK-4105) was used for detection. The sections were counterstained with haematoxylin (Muto Chemicals, Tokyo, Japan: 3000-2), dehydrated and mounted with Multi Mount 480 (Matsunami Glass, Osaka, Japan; FM48001). Negative control staining was performed without primary antibody, as above. Images of immunostained sections were captured by microscopy (Keyence) with a 20×/0.75 PlanApo objective (Olympus). Pax7-positive and -negative nuclei in each field were counted. The percentage of Pax7-positive nuclei in each group was calculated and the results were analysed by one-way ANOVA.

Estimation of oxidant levels and redox active iron

Intracellular oxidant and redox-active iron levels (Kalyanaraman *et al.* 2012) were estimated using modifications of the dichlorodihydrofluorescein diacetate (H_2DCFDA) staining method (Radak *et al.* 2004). In brief, the H_2DCFDA (Invitrogen-Molecular Probes, Carlsbad, CA, USA; no. D399) was dissolved at a concentration of 12.5 mM in ethanol and kept at −80 °C in the dark. The solution was freshly diluted with potassium phosphate buffer to 125 μM before use. For fluorescence reactions, 96-well black microplates were loaded with potassium phosphate buffer (pH 7.4) to a final concentration of 152 μM per well. Then 8 μl diluted tissue homogenates and 40 μl 125 μM dye were added to achieve a final dye concentration of 25 μM. The change in fluorescence intensity was monitored every 5 min for 30 min with excitation and emission wavelengths set at 485 and 538 nm (Fluoroskan Ascent FL). The fluorescence intensity unit was normalized to the protein content and expressed in relative units per minute. This method does not accurately measure the levels of all reactive oxygen species, nor does it directly report hydrogen peroxide levels, but nevertheless increased fluorescence intensity does give an indication of a more oxidizing environment, typically enriched in redox-active iron compounds (Kalyanaraman *et al.* 2012).

Western blots

Whole cell homogenates of the plantaris muscle were generated by Ultra Turrax (IKA-Werke, Staufen, Germany) homogenizer using 10 vol of lysis buffer (137 mM NaCl, 20 mM Tris-HCl, pH 8.0, 2% NP-40, 10% glycerol and protease inhibitors). Ten to 50 μg of protein was electrophoresed on 8–12% (v/v) polyacrylamide SDS-PAGE gels. Proteins were electrotransferred onto PVDF membranes. The membranes were subsequently blocked in 1–5% skimmed milk or BSA, and after blocking, PVDF membranes were incubated at room temperature with primary antibodies [Nampt 1:500 Abcam (Cambridge, MA, USA) no. ab37299, SIRT1 1:3000 Abcam no. ab110304, Acetyl-p53 (Lys373, Lys382) 1:1000 Millipore (Billerica, MA, USA) no. 06-758, Akt 1:1000 Cell Signaling (Danvers, MA, USA) no. 9272, Phospho-Akt (Ser473) 1:1000 Cell Signaling no. 9271, IR-beta 1:1000 Santa Cruz Biotechnology (Santa Cruz, CA, USA) no. sc-711, Myf5 1:5000 Abcam no. ab125078, MyoD 1:1000 Abcam no. ab126726, PCNA 1:500 Santa Cruz no. sc-7907, eNOS 1:625 Abcam no. 76198, VEGF 1:1000 Santa Cruz no. sc-152, GLUT4 1:200 Santa Cruz no. sc-7938, FOXO1 1:1000 Cell Signaling no. 9454, K48-linkage Specific Polyubiquitin 1:1000 Cell Signaling no. 8081S, K63-linkage Specific Polyubiquitin 1:1000 Cell Signaling no. 5621S, MuRF1 1:1000 Santa Cruz no. sc-32920, MuRF2 1:500 Santa Cruz no. sc-49457, Proteasome subunit alpha type-6 (PSMA6) 1:1200 Cell Signaling no. 2459S, Bax 1:500 Santa Cruz no. 492, glyceraldehyde 3-phosphate dehydrogenase (GAPDH) 1:10 000 Sigma-Aldrich (St Louis, MO, USA) no. G8795]. After incubation with primary antibodies, membranes were washed in Tris-buffered saline-Tween-20 (TBST) and incubated with HRP-conjugated secondary antibodies (Jackson ImmunoResearch Europe, Newmarket, UK). After incubation with secondary antibodies, membranes were repeatedly washed. Membranes were incubated with chemiluminescent substrate (Thermo Scientific, Waltham, MA, USA; SuperSignal West Pico Chemiluminescent Substrate no. 34080) and protein bands were visualized on X-ray films. The bands were quantified by ImageJ software, and normalized to GAPDH, which served as an internal control.

Detection of mature miRNAs in skeletal muscle

The TaqMan miRNA reverse transcriptase kit and TaqMan miRNA assays (Applied Biosystems, Foster City, CA, USA) were used to quantify mature miRNA expression levels. Each target miRNA was quantified according to the manufacturer's protocol with minor modifications. Briefly, reverse transcriptase reactions were performed with miRNA-specific reverse transcriptase primers and 5 ng of purified total RNA for 30 min at 16°C, 30 min at 42°C, and finally 5 min at 85°C to heat-inactivate the reverse transcriptase. All volumes suggested in the manufacturer's protocol were halved, as previously reported (Gallagher *et al.* 2010). Real-time PCRs for each miRNA (10 μl total volume) were performed in triplicate, and each 10 μl reaction mixture included 2.4 μl of 10× diluted reverse transcriptase product. Reactions were run on a PRISM 7900HT Fast Real-Time PCR System (Applied Biosystems) at 95°C for 10 min, followed by 40 cycles

at 95°C for 15 s and 60°C for 1 min. Twofold dilution series were performed for all target miRNAs to verify the linearity of the assay. To account for possible differences in the amount of starting RNA, all samples were normalized to the small nuclear RNA RNU48 (catalogue no. 4373383). Importantly, compensatory hypertrophy did not alter RNU48 quantities compared with control values (tested against 18S rRNA). All reactions were run singleplex, in triplicate, and quantified using the cycle threshold ($\Delta\Delta C_t$) method (Livak & Schmittgen, 2001).

Quantitative reverse-transcription PCR validation

Eight miRNAs were selected to investigate their potential role in muscle hypertrophy, using quantitative real-time reverse-transcription PCR (qRT-PCR). TaqMan MicroRNA Assays were used as follows: miR-214, miR-206, miR-23a, miR-34a, miR1, miR-133a, miR-128a and miR-125b. All materials were supplied by Applied Biosystems. Total RNA (10 ng) was reverse transcribed by the MicroRNA Reverse Transcription Kit (Applied Biosystems). qRT-PCR was performed using TaqMan Fast Universal PCR Master Mix on a 7500 Fast Real-Time PCR System according to the manufacturer's protocol. All samples were run in triplicate. Normalized signal levels for each miRNA were calculated using a comparative cycle threshold method (ddCT method of Livak & Schmittgen, 2001) relative to the mean of miR-324-3p and miR-320b following the manufacturer's instructions (SDS Program; Applied Biosystems).

Detection of mRNA levels

RNA isolation. RNA isolation was carried out by the NucleoSpin RNA II kit (Macherey-Nagel, Düren, Germany; no. 740955.250) according to the manufacturer's instructions. Plantaris muscle samples were thawed quickly on ice and added to buffer R1, supplemented with β-mercaptoethanol and disrupted with Ultra Turrax (IKA-Werke) for 60 s at high speed. RNA was eluted by adding 60 μl RNase-free water to columns.

cDNA synthesis. cDNA was synthesized using a Tetro cDNA Synthesis kit (Bioline, Luckenwalde, Germany; no. BIO-65026) in accordance with the manufacturer's instructions. Briefly, the reaction conditions were as follows: 1 μg of RNA, 1 μl of random primers, 1 μl of 10 mM dNTP, 1 μl of RNase inhibitor and 0.25 μl of 200 U μl^{-1} reverse transcriptase in a final volume of 20 μl, and the solution was incubated for 10 min at 25°C, primer annealing, followed by 42°C for 60 min, primer elongation, and followed by 80°C for 5 min termination. cDNA samples were stored at −20°C.

qRT-PCR. Based on the principle of the SybrGreen detection method, EvaGreen dye (Biotium, Hayward, CA, USA) was used to detect PCR products. The PCR was performed using a primer pair specific for mRNA of SIRT1 and IGF-1 isoforms (SIRT1-F: TCTGACTGGA GCTGGGGTTTC, SIRT1-R: GACACAGAGATGGCTGG AACT; IGF1-Ea-F: TTCAGTTCGTGTGTGGACCAAG, IGF1-Ea-R: TCCACAATGCCCGTCTGTGGTG; IGF1-Eb/MGF-F: TCCGCTGCAAGCCTACAAAGTC, IGF1-Eb/MGF-R: CTTTCCTTCTCCTTTGCAGCTTCC). PCR amplifications consisted of equal amounts of template DNA, 10 μl of ImmoMix complete ready-to-use heat-activated 2× reaction mix (Bioline), 1 μl of 20× EvaGreen (Biotium), 2.5 μl of 10 nmol l^{-1} forward and reverse primer (IBAGmbH, Göttingen, Germany) and water to a final volume of 20 μl. Amplifications were performed in a Rotor-Gene 6000 thermal cycler (Corbett Life Science/Qiagen, London, UK) at 95°C for 10 min, followed by 40 cycles of 95°C for 10 s, 60°C for 20 s and 72°C for 30 s in triplicate. The validity of the signal was evaluated by melting analysis and agarose gel electrophoresis. The rat RPL13 gene served as an endogenous control gene.

Assessment of SIRT1 activity

SIRT1 activity was determined using a SIRT1 Fluorometric Kit (Enzo Life Sciences, Plymouth Meeting, PA, USA; no. BML-AK555) (Barbosa *et al.* 2007). Briefly, whole cell lysate from 200 mg plantaris muscle samples was prepared by Dounce homogenizer (12 stokes) in TKMS-NP40 buffer (50 mM Tris-HCl pH 7.4, 25 mM KCl, 5 mM $MgCl_2$, 0.25 mM sucrose, 0.5% NP40). Homogenates were filtered through one sheet of Miracloth filter and sonicated on ice with Sonifier Cell Disruptor B-12 (Branson Sonic Power Company, Danbury, CT, USA) five times for 20 s each. Samples were then centrifuged at 15,000 *g*, for 15 min and supernatant was kept at −80 C for further analysis. Then, 10 μl concentrated sample, 0.5 mM NAD, 1 μl substrate and assay buffer were mixed in a microplate at a final volume of 50 μl and incubated at 30 C for 30 min. Using 1 U per well recombinant, SIRT1 enzyme served as a positive control, while no enzyme was added to the wells of negative controls. Reactions were terminated by the addition of a solution containing Fluor de Lys Developer and 2 mM nicotinamide. Values were determined by reading fluorescence on a fluorometric plate reader (FluoroScan Ascent FL, Thermo Scientific) with an excitation wavelength of 355 nm and emission wavelength of 460 nm. Endogenous SIRT1 activity was determined with the exception that no enzyme was added to the reaction. The data are expressed as a proportion of the total protein content.

NAD/NADH measurement

The measurement was performed by using an NAD/NADH Assay Kit (Abcam no. ab65348) according to the manufacturer's instructions. Briefly, plantaris muscle samples (<10 mg) were homogenized in NADH/NAD extraction buffer and filtered through a 10 kDa Microcon cut off filter, then centrifuged and separated into treated and untreated sample parts. Treated samples underwent a heating procedure at 60°C for 30 min for NAD decomposition. 50 μl diluted NADH standards and samples were loaded into 96-well microplates in duplicate. Then, 100 μl Reaction Mix was added to all wells except the background. After 5 min of incubation at room temperature, 10 μl NADH developer was mixed into the wells to generate colour changes. Optical density was read at 450 nm every 5 min for 1 h. The results were normalized based on the initial tissue weight (Goldspink, 1999).

Statistical analyses

Statistical significance was assessed by the two-sample t test. Correlation matrices were applied to evaluate the relationship between different variables. Significance level was set at $P < 0.05$.

Results

Fourteen days of overload resulted in more than a 40% increase in the mass of the plantaris muscles ($P < 0.01$) (Fig. 1*A*). The actual number of muscle fibres was not changed by hypertrophy (Fig. 1*B*). Satellite cells are proliferating undifferentiated cells, expressing paired-box transcription factors, Pax3 and Pax7. Pax7 genes are crucial to myogenic cells due to their activation of muscle regulatory factors. It has been suggested that growth and repair of skeletal muscle is dependent on Pax7, and the level of Pax7-positive cells increased in the overloaded group (Fig. 1*C*). The levels of myogenic regulatory factor MyoD and proliferating cell nuclear antigen (PCNA), which correlate with DNA synthesis during the cell cycle, were also elevated in the overloaded group ($P < 0.01$) (Fig. 1*D* and *E*).

The increases in muscle hypertrophy were strongly associated with increased levels of SIRT1 mRNA ($P < 0.05$), protein ($P < 0.01$) and activity ($P < 0.01$)

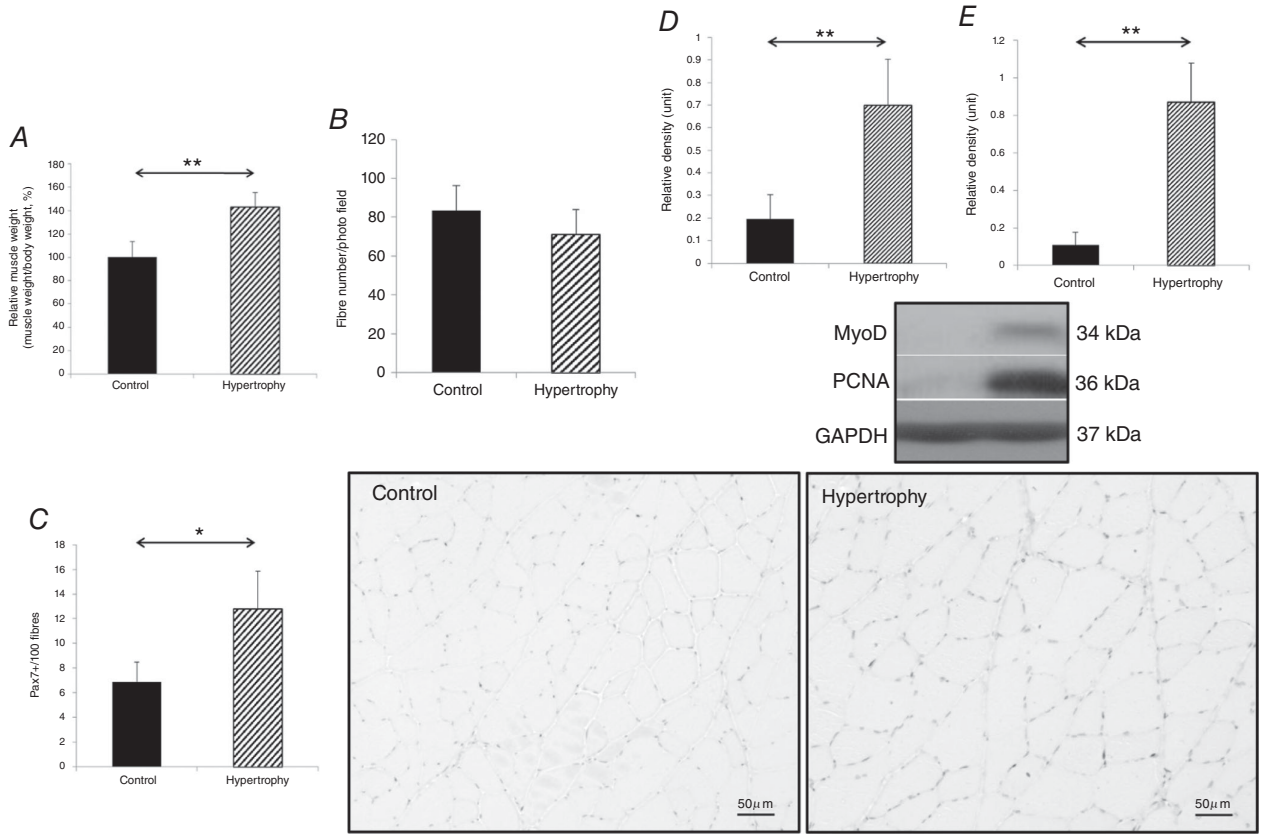

Figure 1. Overload resulted in increased muscle mass, and enhanced levels of MyoD, PCNA and Pax7
Plantaris muscle mass (*A*), number of muscle fibres per photo field (*B*), number of Pax7+ cells/100 fibres (*C*), and MyoD1 (*D*) and PCNA (*E*) protein levels. Results are expressed as mean ± SD (Control: $n = 6$, Hypertrophy: $n = 7$). $^{*}P < 0.05$, $^{**}P < 0.01$.

(Fig. 2*A*–*C*). Concomitantly, the acetylation of p53 decreased significantly ($P < 0.01$), a validating result that would be predicted from the increased SIRT1 levels (Fig. 2*D*). Because Nampt is important for NAD biosynthesis, and because NAD is required for SIRT1 activity, the levels of Nampt were measured and found to increase similarly in the overloaded group as measured relative to activity and protein content of SIRT1 (Fig. 3*A*). Interestingly, NAD levels did not change significantly (Fig. 3*B*), while NADH levels and approximate cellular oxidation state decreased in the overloaded group (Fig. 3*C* and *D*). The crude levels of reactive oxygen species (ROS) was assessed by H_2DCFDA fluorescence (Fig. 3*D*), and the data indicate that the ROS levels are lower 2 weeks after the ablation of soleus and gastrocnemius muscles. The exact measurement of specific ROS is not possible by this method, but the overall assessment of ROS induction can be performed effectively using H_2DCFDA.

The levels of some of the SIRT1 signalling proteins, including Akt1 and eNOS, also increased in the overloaded groups (Fig. 4*A* and *B*). The overload-induced increase in GLUT4 content (Fig. 4*C*) suggests up-regulation of sugar uptake during hypertrophy. On the other hand, overload decreased the levels of FOXO1 and K48 polyubiquitination (Fig. 5*A* and *B*) and increased protein content of proteasome subunit PSMA6 and MuRF2 (Fig. 5*C* and *D*) and K63 ubiquitination (Fig. 5*E*). The level of MuRF1 (Fig. 5*F*) was unchanged by hypertrophy.

The level of miR1, which potentially down-regulates IGF-1 (Hu *et al.* 2013), decreased in the overloaded model (Fig. 6*A*). Indeed, this decrease was associated with increased levels of IGF-1Ea and mechano-growth factor mRNA ($r^2 = -0.818, -0.774$, $P < 0.05$) (Fig. 6*B* and *C*). Along with mechano-growth factor, IGF-1 is important to satellite cell proliferation, differentiation and muscle growth (Allen & Boxhorn, 1989).

The levels of some important miRNAs in control and overloaded skeletal muscles were measured. The data revealed that miR1 and miR133a levels decreased with mechanical overload, while the levels of miR23a, miR34a, miR125b and miR214 increased significantly (Fig. 7). By contrast, the levels of miR128a and miR206 did not change significantly.

Discussion

The present investigation reveals novel information on overload-induced hypertrophy of skeletal muscle. SIRT1

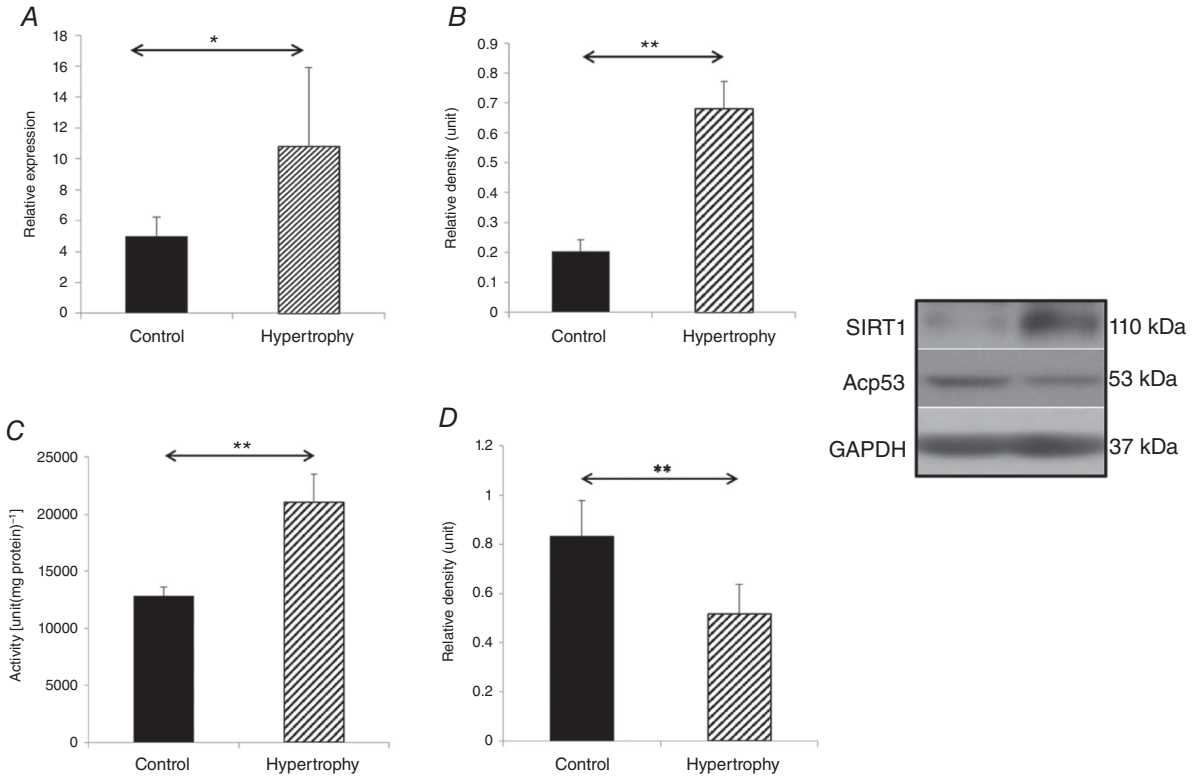

Figure 2. Muscle hypertrophy was associated with increased content and activity of SIRT1
SIRT1 mRNS level (*A*), SIRT1 protein level (*B*), SIRT1 activity (*C*) and Ac-p53 protein level (*D*). Two weeks of compensatory hypertrophy significantly increased the content and activity of SIRT1 and the acetylation level of p53. Results are expressed as mean ± SD (Control: $n = 6$, Hypertrophy: $n = 7$). *$P < 0.05$, **$P < 0.01$.

appears to play an important role in muscle hypertrophy. To our knowledge, there is only one other study which showed that SIRT1 is involved in the hypertrophy of skeletal muscle. In the protocol of Lee & Goldberg (2013) fasting was used to investigate how SIRT1 regulates atrophy-associated genes. The investigators found that after 4 days of fasting, SIRT1 content decreased significantly, and this was associated with increased levels of atrogin1 and MuRF1. On the other hand, when they overexpressed SIRT1 with electroporation, most of the atrogenes were inhibited. Therefore, they concluded that induction of SIRT1 resulted in muscle hypertrophy through the inactivation of downstream FOXOs (Lee & Goldberg, 2013). Our experimental model was very different, as we used compensatory hypertrophy, which increased the mass of the plantaris muscle by some 40%. In our model, the SIRT1 protein content and activity increased significantly in the overloaded muscle along with eNOS and Akt content.

SIRT1 regulates the activity of eNOS and Akt by deacetylation (Mattagajasingh *et al.* 2007; Sundaresan *et al.* 2011) and thus SIRT1 is linked to both NO production

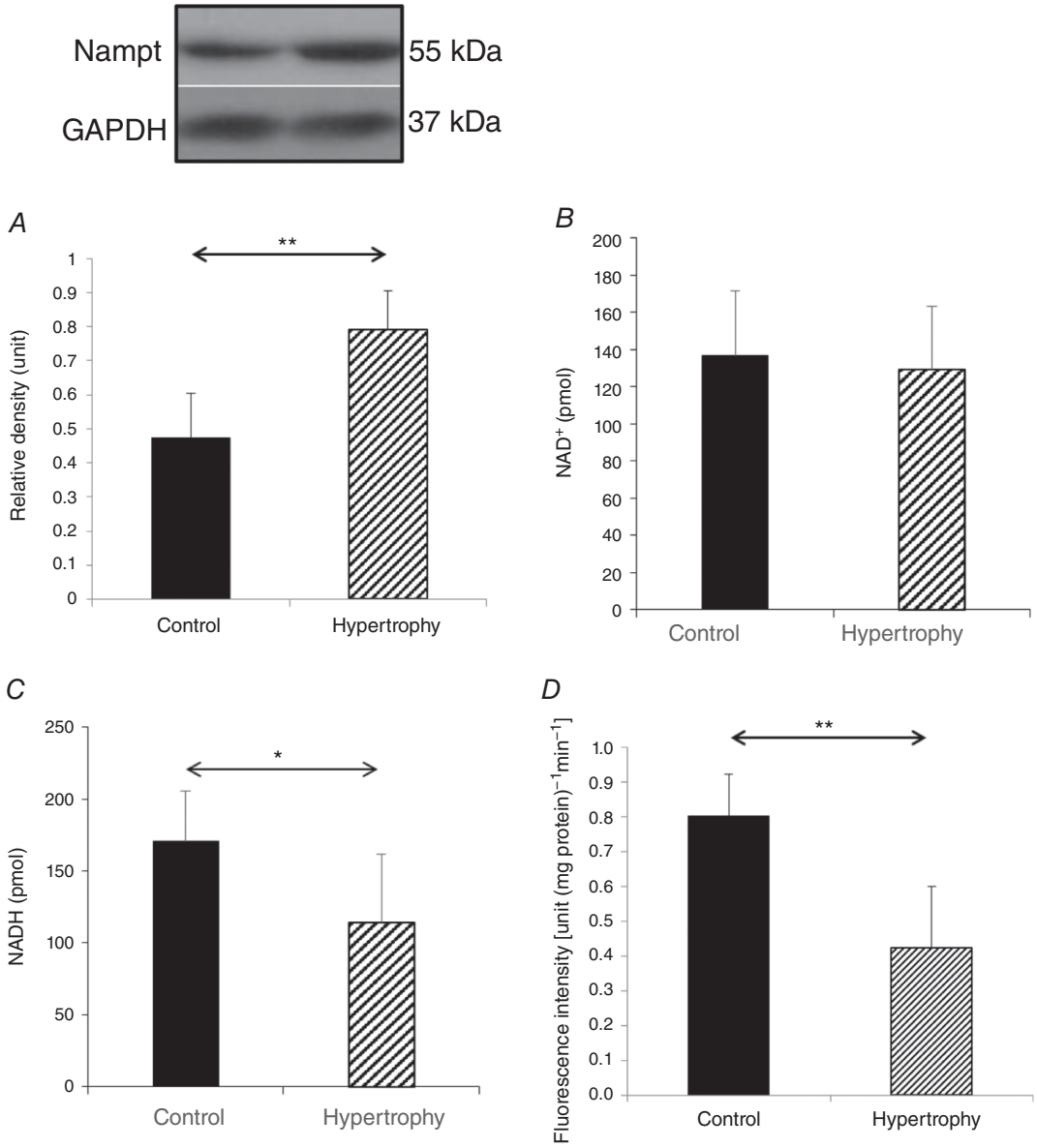

Figure 3. Mechanical overload increased NAMPT and decreased NADH and redox-active iron levels
PBEF/Nampt protein level (*A*), NAD^+ level (*B*), NADH level (*C*) and intracellular oxidant and redox-active iron estimated from dichlorodihydrofluorescein diacetate (H_2DCFDA) fluorescence levels (*D*) can alter the activity of SIRT1. Results are expressed as mean ± SD (Control: $n = 6$, Hypertrophy: $n = 7$). $^*P < 0.05$, $^{**}P < 0.01$.

and protein synthesis. At very low concentrations, NO can actually be regarded as an antioxidant (Lundberg *et al.* 2008) and this could, at least in part, explain why the cellular oxidation level (and redox-active iron) decreased in all overloaded muscles. Lower levels of oxidants result in a reduced redox microenvironment, which has been shown to be beneficial to myogenesis, at least in cell culture (Hansen *et al.* 2007). However, it must be mentioned that the role of various free radicals and other reactive oxygen and nitrogen species in myogenesis could be dependent on the actual levels of such species (Vasilaki & Jackson, 2013). The SIRT1–eNOS interaction may therefore be important to optimize oxidant levels to myogenesis and muscle hypertrophy. Moreover, SIRT1 appears to be important for the activation of cellular growth. Indeed, SIRT1 activates Akt proteins, which appears to have important anti-apoptotic effects (Wang *et al.* 2013). SIRT1 up-regulates genes involved in cell metabolism and growth factor signalling, including Akt (Rafalski *et al.* 2013). Theoretically, reduced apoptosis would help increase muscle mass. Moreover, Akt is not just an activating protein for synthetic pathways, but also suppresses catabolic processes via down-regulation of FOXO1 (Stitt *et al.* 2004). SIRT1 can directly deacetylate FOXO1 and decrease the activity of this protein (Lee & Goldberg, 2013).

Age-related loss of muscle mass is associated with decreased activity of SIRT1 (Koltai *et al.* 2012), and it has been shown that aerobic treadmill running increased the activity of SIRT1 and enhanced anabolic pathways in skeletal muscle (Ziaaldini *et al.* 2015). In accordance with these data, inhibition of poly [ADP-ribose] polymerase (PARP-1) preserved NAD^+ levels in aged skeletal muscle and enhanced the activity of

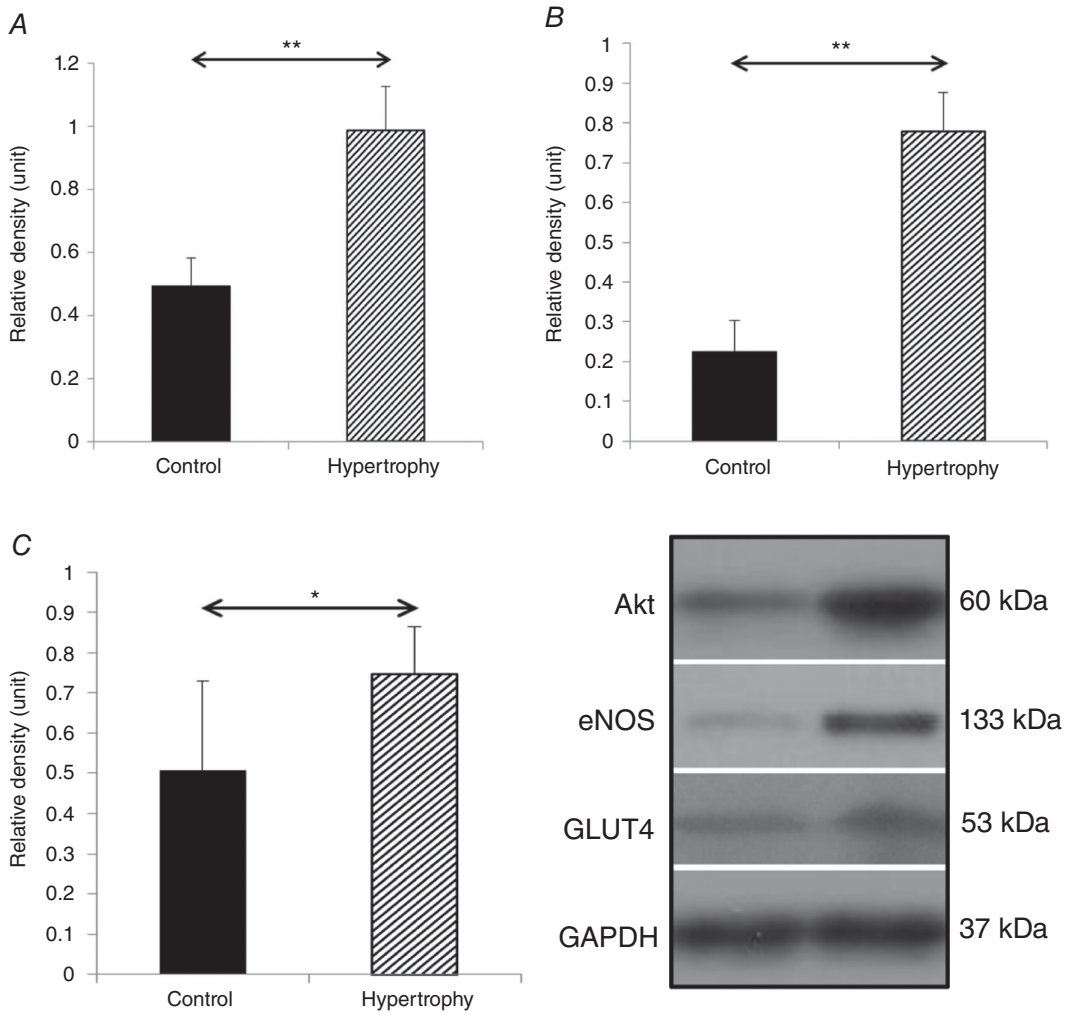

Figure 4. Muscle hypertrophy increased the levels of Akt, eNOS and GLUT4 proteins
Akt (*A*), eNOS (*B*) and GLUT4 (*C*) protein levels can be directly altered by SIRT1 and related to proteins synthesis, redox homeostasis and metabolism. Results are expressed as mean ± SD (Control: $n = 6$, Hypertrophy: $n = 7$). $^*P < 0.05$, $^{**}P < 0.01$.

SIRT1 and resulted in increased mitochondrial biogenesis and performance (Mohamed *et al.* 2014). Moreover, ageing is often associated with increased inflammation and the induction of inducible nitric oxide synthase (iNOS) and *S*-nitrosylation of SIRT1, causing inhibition of this enzyme. Inhibition of SIRT1 activity leads to enhanced acetylation of the p53 and p65 subunits of nuclear factor kappa B (NF-kB), which may be responsible for sarcopenia-associated inflammation (Shinozaki *et al.* 2014).

Muscle atrophy caused by unloading was prevented by resveratrol treatment through activation of SIRT1, attenuating the loss of muscle force (Momken *et al.* 2011). Moreover, resveratrol supplementation in C2C12 cells has been shown to induce hypertrophy through Akt and extracellular signal-regulated kinase (Erk) activation (Montesano *et al.* 2013). SIRT1 activity was not measured in this study, but because resveratrol readily activates SIRT1, it appears that SIRT1 activators are potential pharmacological tools to attenuate muscle atrophy.

SIRT1 is dependent on NAD^+ levels, while the biosynthesis of NAD^+ from nicotinamide (NAM), in mammals, is catalysed by phosphoribosyltransferase (Nampt). It has been shown that depletion of Nampt decreases the levels of SIRT1 (Pillai *et al.* 2005), and therefore Nampt availability is crucial for NAD^+ levels and activity of SIRT1. In the present experimental model, overloading resulted in significant elevation of Nampt levels, suggesting elevated NAD generation. One of the hypotheses for the current investigation was that NO-mediated satellite cell proliferation and then differentiation is necessary for the hypertrophy of skeletal muscle.

Data from genetically modified animal models yielded contrasting results on the role of satellite cells in muscle hypertrophy (Oustanina *et al.* 2004; McCarthy *et al.* 2011). However, even the paper by McCarthy *et al.* (2011), which questions the role of satellite cells in hypertrophy, showed that the ablation of satellite cells halted the increase in myonuclei with hypertrophy and regeneration of fibres. Moreover, it has been shown that SIRT1 stimulates the proliferation of satellite cells (Rathbone *et al.* 2009), which are the primary source of nuclei for skeletal muscle and are required for growth and repair of this tissue (Conboy *et al.* 2005). This observation does not contradict an earlier finding which states that SIRT1 inhibits differentiation of

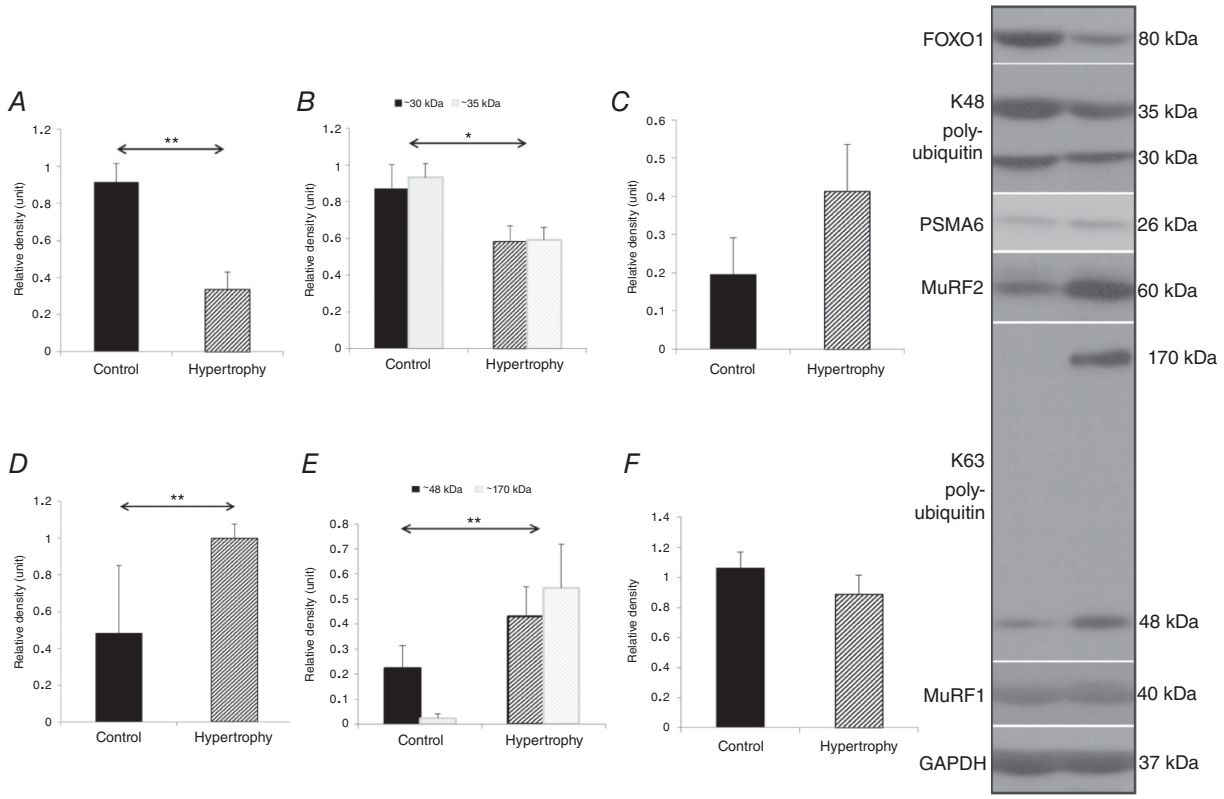

Figure 5. Overload significantly altered the levels of FOXO1, K48 polyubiquitination, PSMA6, MuRF2, K63 polyubiquitination and MuRF1
FOXO1 (*A*), K48 polyubiquitination (*B*), PSMA6 (*C*), MuRF2 (*D*), K63 polyubiquitination (*E*) and MuRF1 (*F*) protein levels can be linked to catabolic process and cell signalling. Results are expressed as mean ± SD (Control: $n = 6$, Hypertrophy: $n = 7$). $^*P < 0.05$, $^{**}P < 0.01$.

satellite cells (Fulco *et al.* 2008), as proliferation is an earlier step in the process of tissue growth and repair.

The differentiation, and the associated increase in protein synthesis, requires a great deal of energy. Therefore, the energy state of the cells could be a limiting factor. Indeed, it has been shown that glucose restriction results in depletion of NAD^+ and Nampt levels and decreased activity of SIRT1, which was associated with impaired myogenesis (Fulco *et al.* 2008). The increased need for energy to cover anabolic processes is supported by the finding that GLUT4 content was increased in our hypertrophy model, in accordance with findings of earlier studies (Kruger *et al.* 2013; Christoffolete *et al.* 2015).

Protein ubiquitination (Ub) could be a marking step for proteasome system-mediated protein degradation. K48-linked Ub chains target proteins to 26S proteasomes, but K63-linked chains are not degraded by proteasomes because the main cellular proteins that associate selectively with K63 chains block their binding to proteasomes (Nathan *et al.* 2013). K48 degradation decreased in the hypertrophied muscle, indicating suppressed degradation, while K63 ubiquitination increased with enhanced muscle mass. Therefore, K68 could serve as a signalling step. X-linked inhibitor of apoptosis protein (XIAP) is considered a legitimate inhibitor of caspases, and cellular IAPs (cIAPs) have been shown to control NF-κB activation (O'Riordan *et al.* 2008). XIAP and cIAP1 conjugate predominantly K63-linked ubiquitin chains to MEKK2 and MEKK3, which results in MEK5–ERK5 interaction, leading to ERK5 inactivation. This observation suggests that K63 of IAP also modulates ERK5–mitogen-activated protein kinase (MAPK) activation and muscle differentiation (Takeda

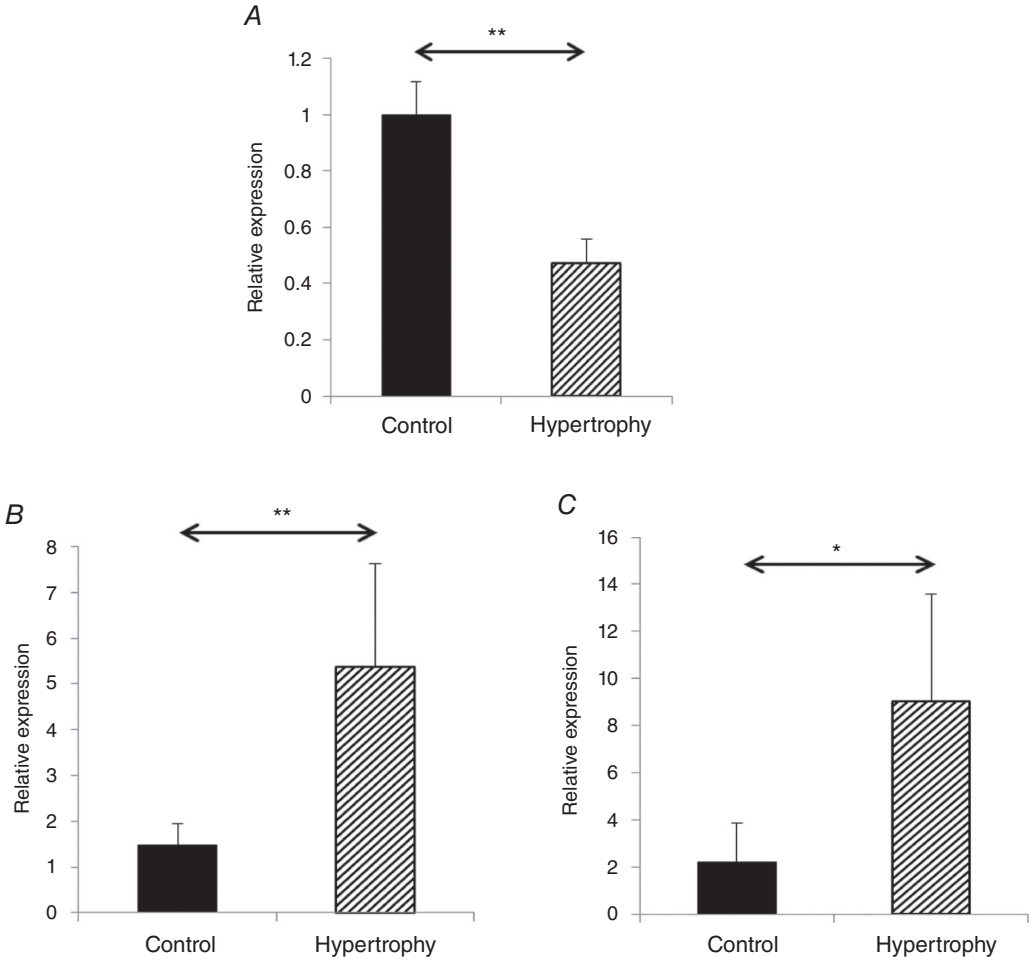

Figure 6. Hypertrophy decreased MiR-1 and increased mRNA of IGF1-Ea and-IGF1-Eb/mechano-growth levels
MiR-1 (*A*) level, IGF1-Ea mRNS level (*B*) and rat-IGF1-Eb/mechano-growth factor mRNS level (*C*). Anabolic process can be activated by IGF-1 family members and miR1 regulates IGF-1. Results are expressed as mean ± SD (Control: $n = 6$, Hypertrophy: $n = 7$). $^*P < 0.05$, $^{**}P < 0.01$.

et al. 2014). Therefore, it cannot be ruled out that the decreases in K48 reflect suppressed degradation and the increases in K63 indicate signalling that could be linked to anabolic processes.

SIRT1 activation has been shown to decrease MuRF1 levels in skeletal muscle (Lee & Goldberg, 2013), a finding that is completely consistent with our current data. Indeed, a functional link is suggested between SIRT1 and MuRF1, because the protective effects of resveratrol on dexamethasone-induced atrogin-1 and MuRF1 expression was eliminated by SIRT1 silencing (Alamdari *et al.* 2012). The increases in MuRF2 levels have been implicated in muscle growth, which agrees with our findings (Shen *et al.* 2011).

A number of miRNAs have distinct expression patterns during muscle differentiation and miRs play regulatory roles in different pathways associated with myogenesis (Ge & Chen, 2011) and possibly in muscle hypertrophy (Rhim *et al.* 2010). We have identified just a few miRs, but the decreases in miR-133a in overloaded muscle fit well with the novel role of SIRT1 in muscle hypertrophy. The miR133a has binding sites for SIRT1 3′ untranslated region, and hence it can down-regulate SIRT1 through its mRNA (Forterre *et al.* 2014). In our compensatory hypertrophy model we found that miR133a levels decreased, suggesting enhanced production of SIRT1, which we indeed measured. In addition, the levels of miR133a were negatively related to Nampt ($r^2 = -0.93$, $P < 0.01$),

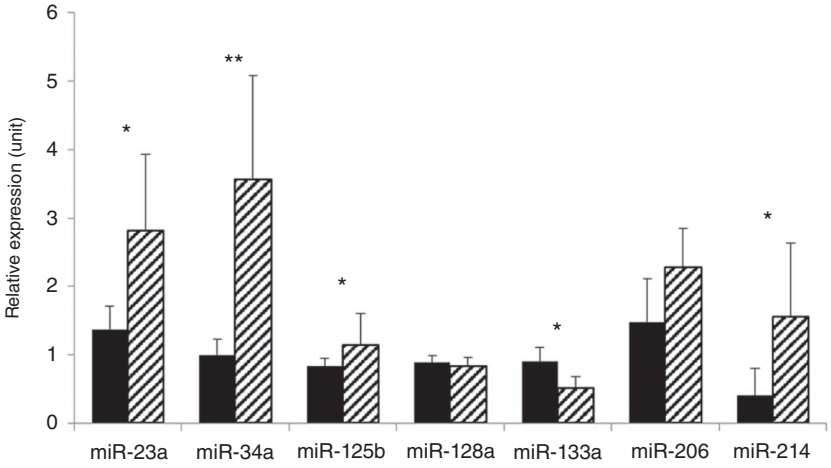

Figure 7. MiR levels were altered by mechanical overload
Muscle-specific miR-23a, miR-34a, miR-125b, miR-133a and miR-214 levels were changed significantly by hypertrophy. Results are expressed as mean ± SD (Control: $n = 6$, Hypertrophy: $n = 7$). $^{*}P < 0.05$, $^{**}P < 0.01$.

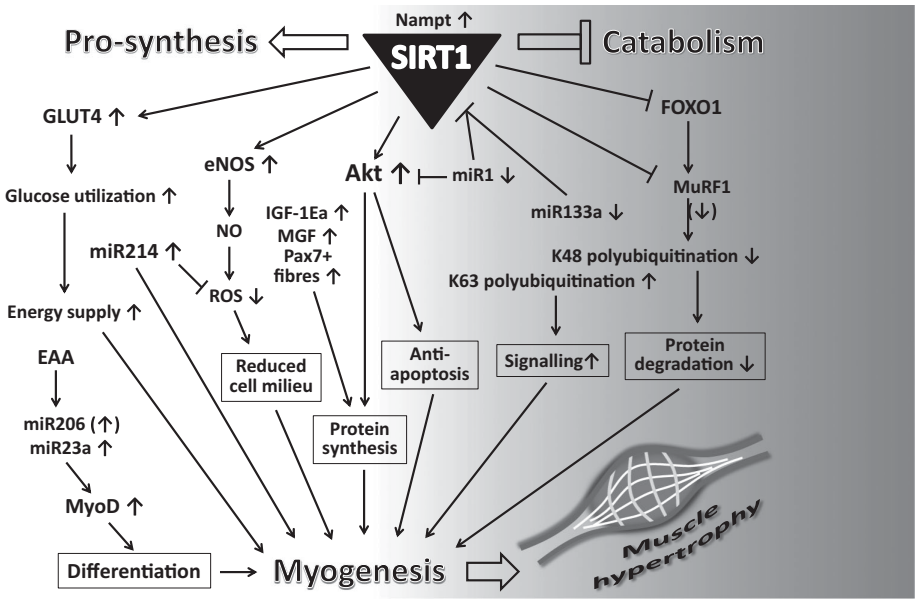

Figure 8. Suggested model of how SIRT1 is involved in the signalling pathways of anabolic and catabolic processes and metabolism in hypertrophy of skeletal muscle

suggesting a possible role for this miR in the NAD salvage pathway.

It has been shown that increased levels of miR1 during atrophy of skeletal muscle reduced HSP70 levels, leading to decreased phosphorylation of Akt (Kukreti *et al.* 2013). In our hypertrophy model, miR1 levels decreased, and we suggest this may indicate that down-regulation of miR1 is important to muscle hypertrophy. This is in accordance with the results of earlier studies (Stantic-Pavlinic & Grcar-Tratnik, 1986; McCarthy & Esser, 2007) using a similar model of muscle hypertrophy.

In addition, it appears that miR1 and miR133a are in the same cluster, which suggests that miR1 can also regulate SIRT1. Indeed, miR1 has a strong negative correlation with muscle mass, IGF-1, SIRT1 and Nampt ($r^2 = -0.993$, -0.818, -0.889, -0.814, $P < 0.05$).

miR-214 is present at high concentrations in embryonic skeletal muscle, but hardly found at all in adult and old skeletal muscle (Huang *et al.* 2008), suggesting that it can play a role in the development of skeletal muscle. Inhibition of miR-214 in C2C12 cell culture curbed the differentiation of myoblasts, and down-regulated levels of myogenin and myosin heavy chain (Feng *et al.* 2011). Here we detected an almost ten-fold increase in miR-214 levels, which could be important in the regulation of overload-induced proliferation and differentiation of skeletal muscle. The results of a recent report suggest that miR-214 can decrease superoxide production via NADPH oxidase 4 (NOX4) (Ma *et al.* 2016). This fits nicely with our results in which we found a negative correlation between miR-214 and H_2DCFDA fluorescence and NADH levels ($r^2 = -0.816$, -0.837, $P < 0.05$), suggesting that miR-214 can modulate the generation of various oxidants during muscle hypertrophy.

Although IGF-1 and mTOR are target genes for miR-128, the expression of miR-128 was not changed in hypertrophied muscle (Chen *et al.* 2016). One possible explanation could be the time course as it cannot be excluded that miR-128 regulation is in the early phase of adaptive response to the ablation of gastrocnemius and soleus muscle. This hypothesis is supported by the finding that this miR has a role in the differentiation of myogenic satellite cells (Harding & Velleman, 2016), which could be an early event of compensatory hypertrophy.

Duchene syndrome is a disease associated with very poor muscle regeneration and hypertrophy and interestingly the miR26-a levels of these patients are down-regulated (Eisenberg *et al.* 2007). The elevation of miR-26a in the hypertrophied muscle did not reach statistical significance ($P = 0.0632$), but the elevation suggests that this miR could also be involved in hypertrophy, probably through the regulation of transforming growth factor.

It has been suggested that essential amino acids (EAAs) stimulate muscle protein synthesis in humans. Increased quantities of EAAs result in increased levels of miR206 and miR23-a in human skeletal muscle, which is associated with elevated levels of MyoD and follistatin, and decreased levels of myostatin (Drummond *et al.* 2009), and these relationships have also been confirmed in the present study.

Our data are consistent with the hypothesis of a novel regulatory role for SIRT1 in overload-induced hypertrophy of skeletal muscle. SIRT1 modulates prosynthetic pathways through eNOS, Akt activation and down-regulation of FOXO1 (Fig. 8). The compensatory hypertrophy of skeletal muscle is regulated by miR1, miR133a, miR23a, miR34a, miR125b and miR214 through modulation of prosynthetic, catabolic and apoptotic pathways. Further functional studies will be needed to directly test our hypothesis that SIRT1 can regulate overload-induced muscle hypertrophy.

References

Alamdari N, Aversa Z, Castillero E, Gurav A, Petkova V, Tizio S & Hasselgren PO (2012). Resveratrol prevents dexamethasone-induced expression of the muscle atrophy-related ubiquitin ligases atrogin-1 and MuRF1 in cultured myotubes through a SIRT1-dependent mechanism. *Biochem Biophys Res Commun* **417**, 528–533.

Allen RE & Boxhorn LK (1989). Regulation of skeletal muscle satellite cell proliferation and differentiation by transforming growth factor-β, insulin-like growth factor I, and fibroblast growth factor. *J Cell Physiol* **138**, 311–315.

Anderson JE (2000). A role for nitric oxide in muscle repair: nitric oxide-mediated activation of muscle satellite cells. *Mol Biol Cell* **11**, 1859–1874.

Baldwin KM, Valdez V, Herrick RE, MacIntosh AM & Roy RR (1982). Biochemical properties of overloaded fast-twitch skeletal muscle. *J Appl Physiol Respir Environ Exerc Physiol* **52**, 467–472.

Banerjee J, Bruckbauer A & Zemel MB (2016). Activation of the AMPK/Sirt1 pathway by a leucine–metformin combination increases insulin sensitivity in skeletal muscle, and stimulates glucose and lipid metabolism and increases life span in *Caenorhabditis elegans*. *Metabolism* **65**, 1679–1691.

Barbosa MT, Soares SM, Novak CM, Sinclair D, Levine JA, Aksoy P & Chini EN (2007). The enzyme CD38 (a NAD glycohydrolase, EC 3.2.2.5) is necessary for the development of diet-induced obesity. *FASEB J* **21**, 3629–3639.

Bigard AX, Zoll J, Ribera F, Mateo P, Sanchez H, Serrurier B & Ventura-Clapier R (2001). Influence of overload on phenotypic remodeling in regenerated skeletal muscle. *Am J Physiol Cell Physiol* **281**, C1686–1694.

Buler M, Andersson U & Hakkola J (2016). Who watches the watchmen? Regulation of the expression and activity of sirtuins. *FASEB J* **30**, 3942–3960.

Canto C, Gerhart-Hines Z, Feige JN, Lagouge M, Noriega L, Milne JC, Elliott PJ, Puigserver P & Auwerx J (2009). AMPK regulates energy expenditure by modulating NAD+ metabolism and SIRT1 activity. *Nature* **458**, 1056–1060.

Chaillou T, Koulmann N, Simler N, Meunier A, Serrurier B, Chapot R, Peinnequin A, Beaudry M & Bigard X (2012). Hypoxia transiently affects skeletal muscle hypertrophy in a functional overload model. *Am J Physiol Regul Integr Comp Physiol* **302**, R643–654.

Chen PH, Cheng CH, Shih CM, Ho KH, Lin CW, Lee CC, Liu AJ, Chang CK & Chen KC (2016). The inhibition of microRNA-128 on IGF-1-activating mTOR signaling involves in temozolomide-induced glioma cell apoptotic death. *PLoS One* **11**, e0167096.

Christoffolete MA, Silva WJ, Ramos GV, Bento MR, Costa MO, Ribeiro MO, Okamoto MM, Lohmann TH, Machado UF, Musaro A & Moriscot AS (2015). Muscle IGF-1-induced skeletal muscle hypertrophy evokes higher insulin sensitivity and carbohydrate use as preferential energy substrate. *Biomed Res Int* **2015**, 282984.

Conboy IM, Conboy MJ, Wagers AJ, Girma ER, Weissman IL & Rando TA (2005). Rejuvenation of aged progenitor cells by exposure to a young systemic environment. *Nature* **433**, 760–764.

Csiszar A, Labinskyy N, Pinto JT, Ballabh P, Zhang H, Losonczy G, Pearson K, de Cabo R, Pacher P, Zhang C & Ungvari Z (2009). Resveratrol induces mitochondrial biogenesis in endothelial cells. *Am J Physiol Heart Circ Physiol* **297**, H13–20.

Davies KJ, Packer L & Brooks GA (1981). Biochemical adaptation of mitochondria, muscle, and whole-animal respiration to endurance training. *Arch Biochem Biophys* **209**, 539–554.

Drummond MJ, Glynn EL, Fry CS, Dhanani S, Volpi E & Rasmussen BB (2009). Essential amino acids increase microRNA-499, -208b, and -23a and downregulate myostatin and myocyte enhancer factor 2C mRNA expression in human skeletal muscle. *J Nutr* **139**, 2279–2284.

Eisenberg I, Eran A, Nishino I, Moggio M, Lamperti C, Amato AA, Lidov HG, Kang PB, North KN, Mitrani-Rosenbaum S, Flanigan KM, Neely LA, Whitney D, Beggs AH, Kohane IS & Kunkel LM (2007). Distinctive patterns of microRNA expression in primary muscular disorders. *Proc Natl Acad Sci USA* **104**, 17016–17021.

Feng Y, Cao JH, Li XY & Zhao SH (2011). Inhibition of miR-214 expression represses proliferation and differentiation of C2C12 myoblasts. *Cell Biochem Funct* **29**, 378–383.

Forterre A, Jalabert A, Chikh K, Pesenti S, Euthine V, Granjon A, Errazuriz E, Lefai E, Vidal H & Rome S (2014). Myotube-derived exosomal miRNAs downregulate Sirtuin1 in myoblasts during muscle cell differentiation. *Cell Cycle* **13**, 78–89.

Fulco M, Cen Y, Zhao P, Hoffman EP, McBurney MW, Sauve AA & Sartorelli V (2008). Glucose restriction inhibits skeletal myoblast differentiation by activating SIRT1 through AMPK-mediated regulation of Nampt. *Dev Cell* **14**, 661–673.

Gallagher IJ, Scheele C, Keller P, Nielsen AR, Remenyi J, Fischer CP, Roder K, Babraj J, Wahlestedt C, Hutvagner G, Pedersen BK & Timmons JA (2010). Integration of microRNA changes in vivo identifies novel molecular features of muscle insulin resistance in type 2 diabetes. *Genome Med* **2**, 9.

Ge Y & Chen J (2011). MicroRNAs in skeletal myogenesis. *Cell Cycle* **10**, 441–448.

Goldspink G (1999). Changes in muscle mass and phenotype and the expression of autocrine and systemic growth factors by muscle in response to stretch and overload. *J Anat* **194**, 323–334.

Grundy D (2015). Principles and standards for reporting animal experiments in *The Journal of Physiology* and *Experimental Physiology*. *J Physiol* **593**, 2547–2549.

Han GD, Zhang S, Marshall DJ, Ke CH & Dong YW (2013). Metabolic energy sensors (AMPK and SIRT1), protein carbonylation and cardiac failure as biomarkers of thermal stress in an intertidal limpet: linking energetic allocation with environmental temperature during aerial emersion. *J Exp Biol* **216**, 3273–3282.

Hansen JM, Klass M, Harris C & Csete M (2007). A reducing redox environment promotes C2C12 myogenesis: implications for regeneration in aged muscle. *Cell Biol Int* **31**, 546–553.

Harding RL & Velleman SG (2016). MicroRNA regulation of myogenic satellite cell proliferation and differentiation. *Mol Cell Biochem* **412**, 181–195.

Holloszy JO (1967). Biochemical adaptations in muscle. Effects of exercise on mitochondrial oxygen uptake and respiratory enzyme activity in skeletal muscle. *J Biol Chem* **242**, 2278–2282.

Hu W, Meng X, Lu T, Wu L, Li T, Li M & Tian Y (2013). MicroRNA1 inhibits the proliferation of Chinese sika deerderived cartilage cells by binding to the 3'-untranslated region of IGF1. *Mol Med Rep* **8**, 523–528.

Huang TH, Zhu MJ, Li XY & Zhao SH (2008). Discovery of porcine microRNAs and profiling from skeletal muscle tissues during development. *PLoS One* **3**, e3225.

Igarashi M & Guarente L (2016). mTORC1 and SIRT1 cooperate to foster expansion of gut adult stem cells during calorie restriction. *Cell* **166**, 436–450.

Kalyanaraman B, Darley-Usmar V, Davies KJA, Dennery P, Forman HJ, Grisham M, Mann G, Moor, Roberts JLJI & Ischiropoulos H (2012). Measuring reactive oxygen and nitrogen species with fluorescent probles: challenges and limtations. *Free Radic BiolMed* **52**, 1–6.

Koltai E, Hart N, Taylor AW, Goto S, Ngo JK, Davies KJ & Radak Z (2012). Age-associated declines in mitochondrial biogenesis and protein quality control factors are minimized by exercise training. *Am J Physiol Regul Integr Comp Physiol* **303**, R127–134.

Kruger K, Gessner DK, Seimetz M, Banisch J, Ringseis R, Eder K, Weissmann N & Mooren FC (2013). Functional and muscular adaptations in an experimental model for isometric strength training in mice. *PLoS One* **8**, e79069.

Kukreti H, Amuthavalli K, Harikumar A, Sathiyamoorthy S, Feng PZ, Anantharaj R, Tan SL, Lokireddy S, Bonala S, Sriram S, McFarlane C, Kambadur R & Sharma M (2013). Muscle-specific microRNA1 (miR1) targets heat shock protein 70 (HSP70) during dexamethasone-mediated atrophy. *J Biol Chem* **288**, 6663–6678.

Lee D & Goldberg AL (2013). SIRT1 protein, by blocking the activities of transcription factors FoxO1 and FoxO3, inhibits muscle atrophy and promotes muscle growth. *J Biol Chem* **288**, 30515–30526.

Lee SJ & McPherron AC (2001). Regulation of myostatin activity and muscle growth. *Proc Natl Acad Sci USA* **98**, 9306–9311.

Livak KJ & Schmittgen TD (2001). Analysis of relative gene expression data using real-time quantitative PCR and the $2^{-\Delta\Delta C(T)}$ method. *Methods* **25**, 402–408.

Lu L, Zhou L, Chen EZ, Sun K, Jiang P, Wang L, Su X, Sun H & Wang H (2012). A novel YY1-miR-1 regulatory circuit in skeletal myogenesis revealed by genome-wide prediction of YY1-miRNA network. *PLoS One* **7**, e27596.

Lundberg JO, Weitzberg E & Gladwin MT (2008). The nitrate–nitrite–nitric oxide pathway in physiology and therapeutics. *Nat Rev Drug Discov* **7**, 156–167.

Ma W, Li J, Hu J, Cheng Y, Wang J, Zhang X & Xu M (2016). miR214-regulated p53-NOX4/p66shc pathway plays a crucial role in the protective effect of Ginkgolide B against cisplatin-induced cytotoxicity in HEI-OC1 cells. *Chem Biol Interact* **245**, 72–81.

Marton O, Koltai E, Takeda M, Koch LG, Britton SL, Davies KJ, Boldogh I & Radak Z (2015). Mitochondrial biogenesis-associated factors underlie the magnitude of response to aerobic endurance training in rats. *Pflugers Arch* **467**, 779–788.

Mattagajasingh I, Kim CS, Naqvi A, Yamamori T, Hoffman TA, Jung SB, DeRicco J, Kasuno K & Irani K (2007). SIRT1 promotes endothelium-dependent vascular relaxation by activating endothelial nitric oxide synthase. *Proc Natl Acad Sci USA* **104**, 14855–14860.

McCarthy JJ & Esser KA (2007). MicroRNA-1 and microRNA-133a expression are decreased during skeletal muscle hypertrophy. *J Appl Physiol (1985)* **102**, 306–313.

McCarthy JJ, Mula J, Miyazaki M, Erfani R, Garrison K, Farooqui AB, Srikuea R, Lawson BA, Grimes B, Keller C, Van Zant G, Campbell KS, Esser KA, Dupont-Versteegden EE & Peterson CA (2011). Effective fiber hypertrophy in satellite cell-depleted skeletal muscle. *Development* **138**, 3657–3666.

Mohamed JS, Wilson JC, Myers MJ, Sisson KJ & Alway SE (2014). Dysregulation of SIRT-1 in aging mice increases skeletal muscle fatigue by a PARP-1-dependent mechanism. *Aging (Albany NY)* **6**, 820–834.

Momken I, Stevens L, Bergouignan A, Desplanches D, Rudwill F, Chery I, Zahariev A, Zahn S, Stein TP, Sebedio JL, Pujos-Guillot E, Falempin M, Simon C, Coxam V, Andrianjafiniony T, Gauquelin-Koch G, Picquet F & Blanc S (2011). Resveratrol prevents the wasting disorders of mechanical unloading by acting as a physical exercise mimetic in the rat. *FASEB J* **25**, 3646–3660.

Montesano A, Luzi L, Senesi P, Mazzocchi N & Terruzzi I (2013). Resveratrol promotes myogenesis and hypertrophy in murine myoblasts. *J Transl Med* **11**, 310.

Nathan JA, Kim HT, Ting L, Gygi SP & Goldberg AL (2013). Why do cellular proteins linked to K63-polyubiquitin chains not associate with proteasomes? *EMBO J* **32**, 552–565.

Nedachi T, Kadotani A, Ariga M, Katagiri H & Kanzaki M (2008). Ambient glucose levels qualify the potency of insulin myogenic actions by regulating SIRT1 and FoxO3a in C2C12 myocytes. *Am J Physiol Endocrinol Metab* **294**, E668–678.

O'Riordan MX, Bauler LD, Scott FL & Duckett CS (2008). Inhibitor of apoptosis proteins in eukaryotic evolution and development: a model of thematic conservation. *Dev Cell* **15**, 497–508.

Ouchi N, Oshima Y, Ohashi K, Higuchi A, Ikegami C, Izumiya Y & Walsh K (2008). Follistatin-like 1, a secreted muscle protein, promotes endothelial cell function and revascularization in ischemic tissue through a nitric-oxide synthase-dependent mechanism. *J Biol Chem* **283**, 32802–32811.

Oustanina S, Hause G & Braun T (2004). Pax7 directs postnatal renewal and propagation of myogenic satellite cells but not their specification. *EMBO J* **23**, 3430–3439.

Pillai JB, Isbatan A, Imai S & Gupta MP (2005). Poly(ADP-ribose) polymerase-1-dependent cardiac myocyte cell death during heart failure is mediated by NAD+ depletion and reduced Sir2α deacetylase activity. *J Biol Chem* **280**, 43121–43130.

Pisconti A, Brunelli S, Di Padova M, De Palma C, Deponti D, Baesso S, Sartorelli V, Cossu G & Clementi E (2006). Follistatin induction by nitric oxide through cyclic GMP: a tightly regulated signaling pathway that controls myoblast fusion. *J Cell Biol* **172**, 233–244.

Radak Z, Chung HY, Naito H, Takahashi R, Jung KJ, Kim HJ & Goto S (2004). Age-associated increase in oxidative stress and nuclear factor kappaB activation are attenuated in rat liver by regular exercise. *FASEB J* **18**, 749–750.

Rafalski VA, Ho PP, Brett JO, Ucar D, Dugas JC, Pollina EA, Chow LM, Ibrahim A, Baker SJ, Barres BA, Steinman L & Brunet A (2013). Expansion of oligodendrocyte progenitor cells following SIRT1 inactivation in the adult brain. *Nat Cell Biol* **15**, 614–624.

Rao PK, Kumar RM, Farkhondeh M, Baskerville S & Lodish HF (2006). Myogenic factors that regulate expression of muscle-specific microRNAs. *Proc Natl Acad Sci USA* **103**, 8721–8726.

Rathbone CR, Booth FW & Lees SJ (2009). Sirt1 increases skeletal muscle precursor cell proliferation. *Eur J Cell Biol* **88**, 35–44.

Rhim C, Cheng CS, Kraus WE & Truskey GA (2010). Effect of microRNA modulation on bioartificial muscle function. *Tissue Eng Part A* **16**, 3589–3597.

Rosenberg MI, Georges SA, Asawachaicharn A, Analau E & Tapscott SJ (2006). MyoD inhibits Fstl1 and Utrn expression by inducing transcription of miR-206. *J Cell Biol* **175**, 77–85.

Ruas JL, White JP, Rao RR, Kleiner S, Brannan KT, Harrison BC, Greene NP, Wu J, Estall JL, Irving BA, Lanza IR, Rasbach KA, Okutsu M, Nair KS, Yan Z, Leinwand LA & Spiegelman BM (2012). A PGC-1α isoform induced by resistance training regulates skeletal muscle hypertrophy. *Cell* **151**, 1319–1331.

Ryall JG, Dell'Orso S, Derfoul A, Juan A, Zare H, Feng X, Clermont D, Koulnis M, Gutierrez-Cruz G, Fulco M & Sartorelli V (2015). The NAD^+-dependent SIRT1 deacetylase translates a metabolic switch into regulatory epigenetics in skeletal muscle stem cells. *Cell Stem Cell* **16**, 171–183.

Scheffler TL, Scheffler JM, Park S, Kasten SC, Wu Y, McMillan RP, Hulver MW, Frisard MI & Gerrard DE (2014). Fiber hypertrophy and increased oxidative capacity can occur simultaneously in pig glycolytic skeletal muscle. *Am J Physiol Cell Physiol* **306**, C354–363.

Shen H, Zhao SH, Cao JH, Li XY & Fan B (2011). Porcine MuRF2 and MuRF3: molecular cloning, expression and association analysis with muscle production traits. *Mol Biol Rep* **38**, 5115–5123.

Shepstone TN, Tang JE, Dallaire S, Schuenke MD, Staron RS & Phillips SM (2005). Short-term high- vs. low-velocity isokinetic lengthening training results in greater hypertrophy of the elbow flexors in young men. *J Appl Physiol (1985)* **98**, 1768–1776.

Shinozaki S, Chang K, Sakai M, Shimizu N, Yamada M, Tanaka T, Nakazawa H, Ichinose F, Yamada Y, Ishigami A, Ito H, Ouchi Y, Starr ME, Saito H, Shimokado K, Stamler JS & Kaneki M (2014). Inflammatory stimuli induce inhibitory *S*-nitrosylation of the deacetylase SIRT1 to increase acetylation and activation of p53 and p65. *Sci Signal* **7**, ra106.

Stantic-Pavlinic M & Grcar-Tratnik M (1986). [Clinical observations in tick-borne meningoencephalitis]. *Vojnosanit Pregl* **43**, 340–342.

Stitt TN, Drujan D, Clarke BA, Panaro F, Timofeyva Y, Kline WO, Gonzalez M, Yancopoulos GD & Glass DJ (2004). The IGF-1/PI3K/Akt pathway prevents expression of muscle atrophy-induced ubiquitin ligases by inhibiting FOXO transcription factors. *Mol Cell* **14**, 395–403.

Sundaresan NR, Pillai VB, Wolfgeher D, Samant S, Vasudevan P, Parekh V, Raghuraman H, Cunningham JM, Gupta M & Gupta MP (2011). The deacetylase SIRT1 promotes membrane localization and activation of Akt and PDK1 during tumorigenesis and cardiac hypertrophy. *Sci Signal* **4**, ra46.

Takeda AN, Oberoi-Khanuja TK, Glatz G, Schulenburg K, Scholz RP, Carpy A, Macek B, Remenyi A & Rajalingam K (2014). Ubiquitin-dependent regulation of MEKK2/3-MEK5-ERK5 signaling module by XIAP and cIAP1. *EMBO J* **33**, 1784–1801.

Tang AH & Rando TA (2014). Induction of autophagy supports the bioenergetic demands of quiescent muscle stem cell activation. *EMBO J* **33**, 2782–2797.

Vasilaki A & Jackson MJ (2013). Role of reactive oxygen species in the defective regeneration seen in aging muscle. *Free Radic Biol Med* **65**, 317–323.

Viles JM & Powell EC (1981). Myofiber damage accompanying intramuscular parasitism by *Sarcocystis muris*. *Tissue Cell* **13**, 45–60.

Wang D, Hu Z, Hao J, He B, Gan Q, Zhong X, Zhang X, Shen J, Fang J & Jiang W (2013). SIRT1 inhibits apoptosis of degenerative human disc nucleus pulposus cells through activation of Akt pathway. *Age (Dordr)* **35**, 1741–1753.

Yoshioka T, Inagaki K, Noguchi T, Sakai M, Ogawa W, Hosooka T, Iguchi H, Watanabe E, Matsuki Y, Hiramatsu R & Kasuga M (2009). Identification and characterization of an alternative promoter of the human PGC-1α gene. *Biochem Biophys Res Commun* **381**, 537–543.

Ziaaldini MM, Koltai E, Csende Z, Goto S, Boldogh I, Taylor AW & Radak Z (2015). Exercise training increases anabolic and attenuates catabolic and apoptotic processes in aged skeletal muscle of male rats. *Exp Gerontol* **67**, 9–14.

Additional information

Competing interests

No conflicting interests.

Author contributions

Z.R., E.K., I.B., K.J.D., H.D., E.C.F. and H.N. conceived and designed the study; E.K., C.C., Z.B. and S.M. performed the experiments; E.K., Z.B. and Z.M. analysed the data; Z.R., E.K., K.J.D. and I.B. interpreted the results; Z.R., E.K., H.N. and K.J.D. drafted the manuscript; Z.R., E.K., H.D., E.C.F., Z.M. and K.J.D. edited and revised the manuscript. All authors approved the final version of the manuscript. Experimental procedures were performed in the University of Physical Education, Hungary, and in Juntendo University, Japan.

Funding

This study was supported by an International Collaboration Grant by the National Strength and Conditioning Association awarded to A.F and Z.R. and an OTKA grant (112810) awarded to Z.R. E.K. was the recipient of a Bolyai Janos fellowship from The Hungarian Academy of Science. K.J.A.D. was supported by grant no. ES003598 from the US National Institutes of Health/National Institute of Environmental Health Sciences.